DETERMINE PLANE-OF-SKY MAGNETIC FIELD DIRECTION VIA MOLECULAR LINE POLARIZATION

Tao-Chung Ching[1], Jansky Fellow

Zhi-Yun Li[2], Qizhou Zhang[3], Josep M. Girart[4], Chin-Fei Lee[5], Shih-Ping Lai[6], Ramprasad Rao[3], Emmanuel Momjian[1]

1. National Radio Astronomy Observatory, USA 2. University of Virginia, USA 3. Harvard-Smithsonian Center for Astrophysics, USA 4. Institut de Ciencies de l'Espai, CSIC-IEEC, Spain 5. ASIAA, Taiwan 6. National Tsing-Hua University, Taiwan

Braking B Field in Star Formation

- Magnetic field is frozen in ideal MHD
- Magnetic flux must be reduced to enable star formation
- Magnetic braking is needed to remove angular momentum

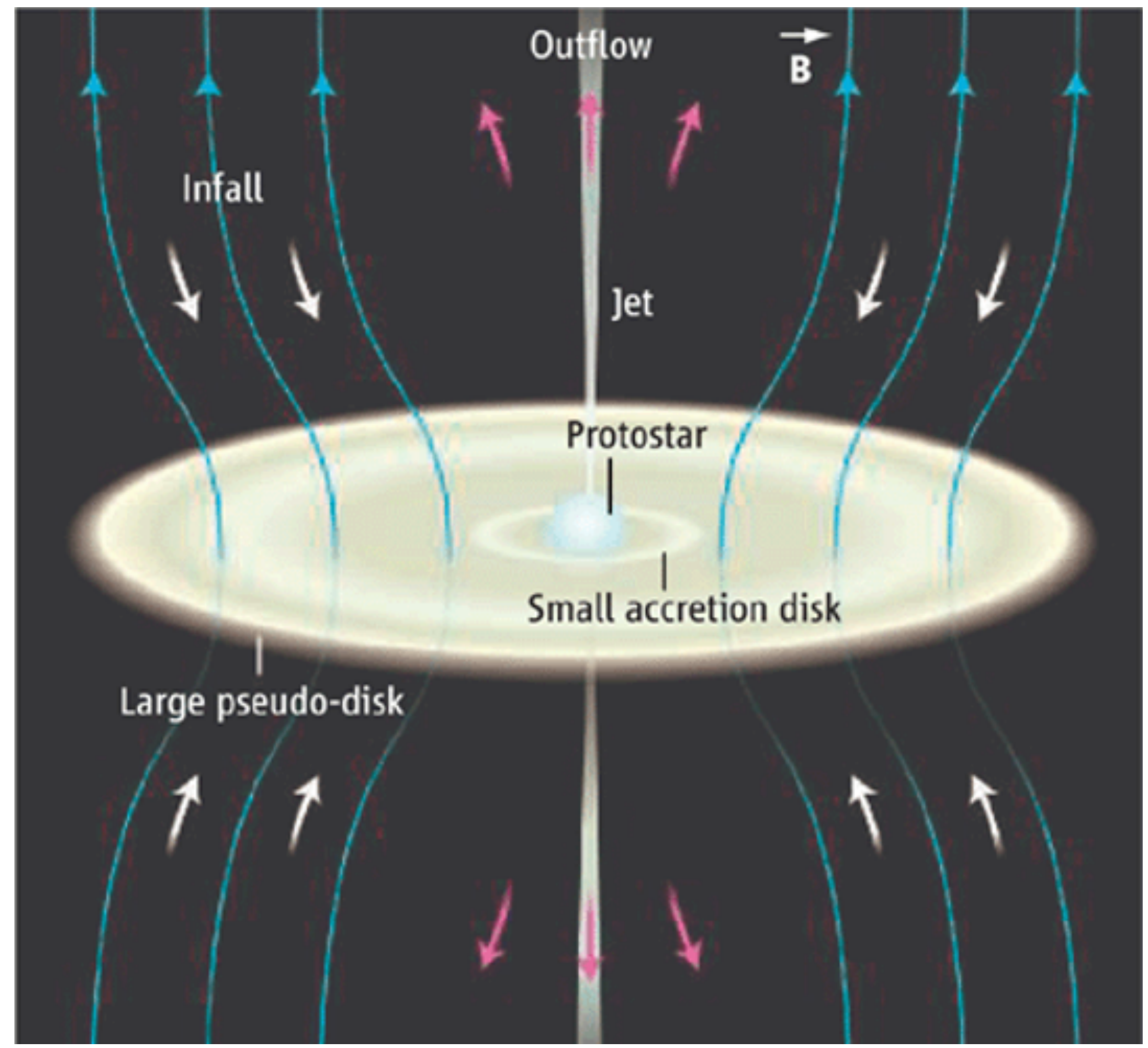

Crutcher 2006

Galactic Magnetic Field Surveys

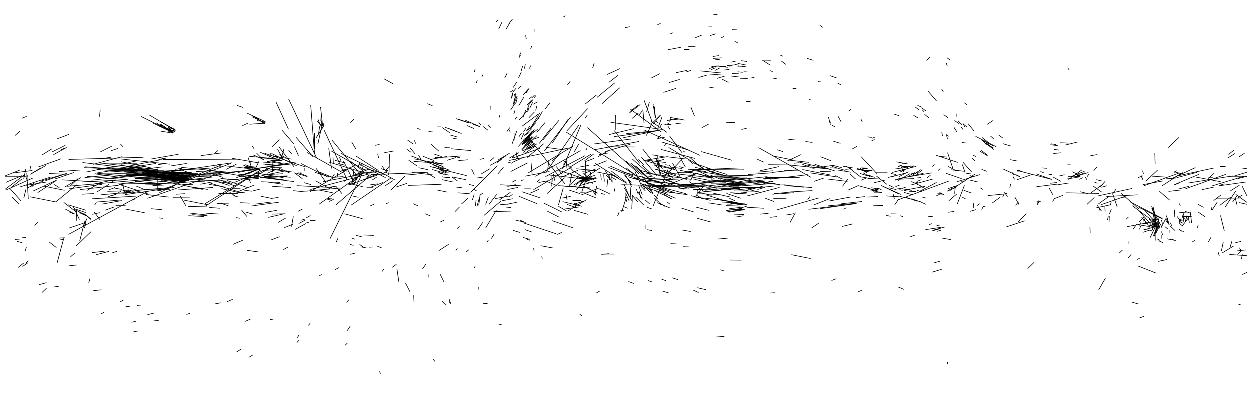

Optical polarization, 9286 stars, Heiles 2000

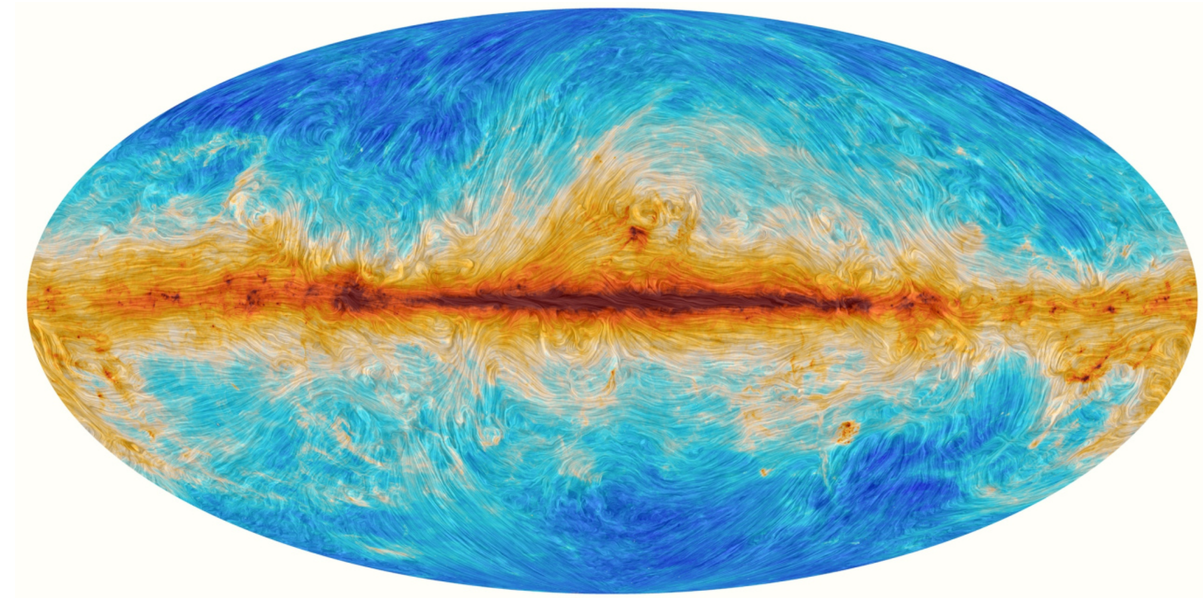

Dust polarization, Planck XXXV 2015

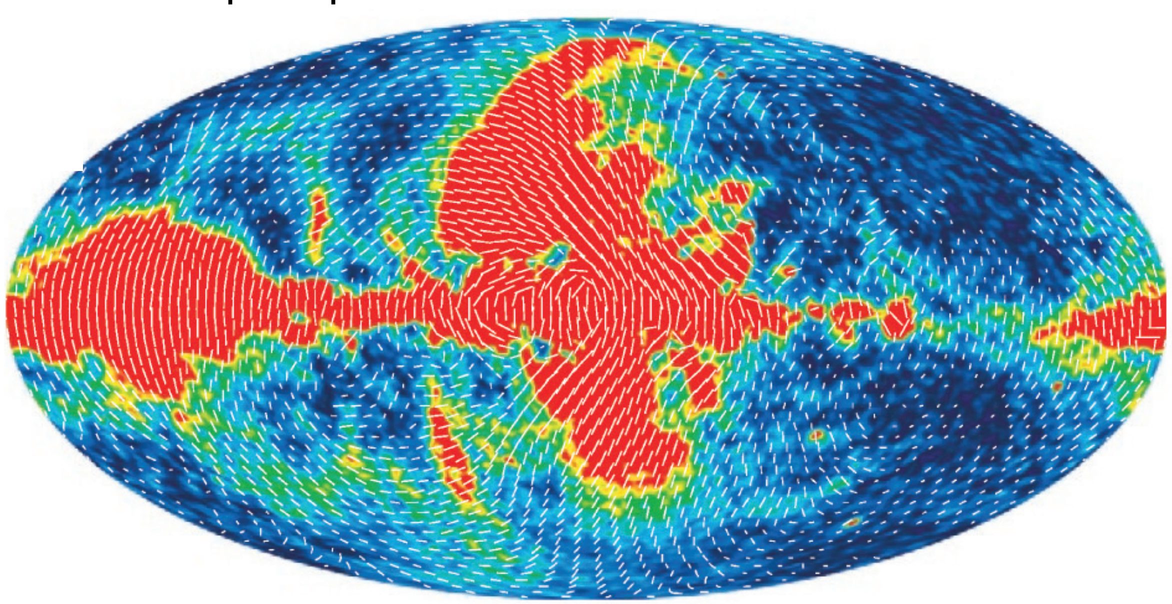

Synchrotron polarization at 23 GHz, Bennett et al. 2013

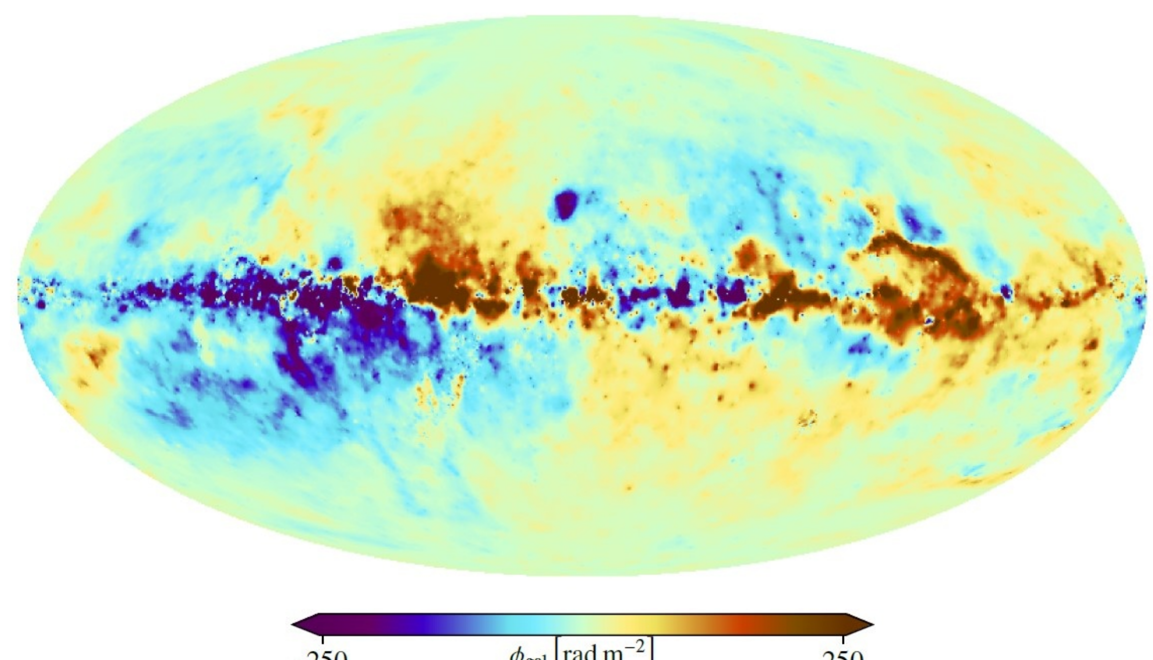

55190 RMs, Hutschenreuter et al. 2021

What's Plane-of-sky B Field Direction?

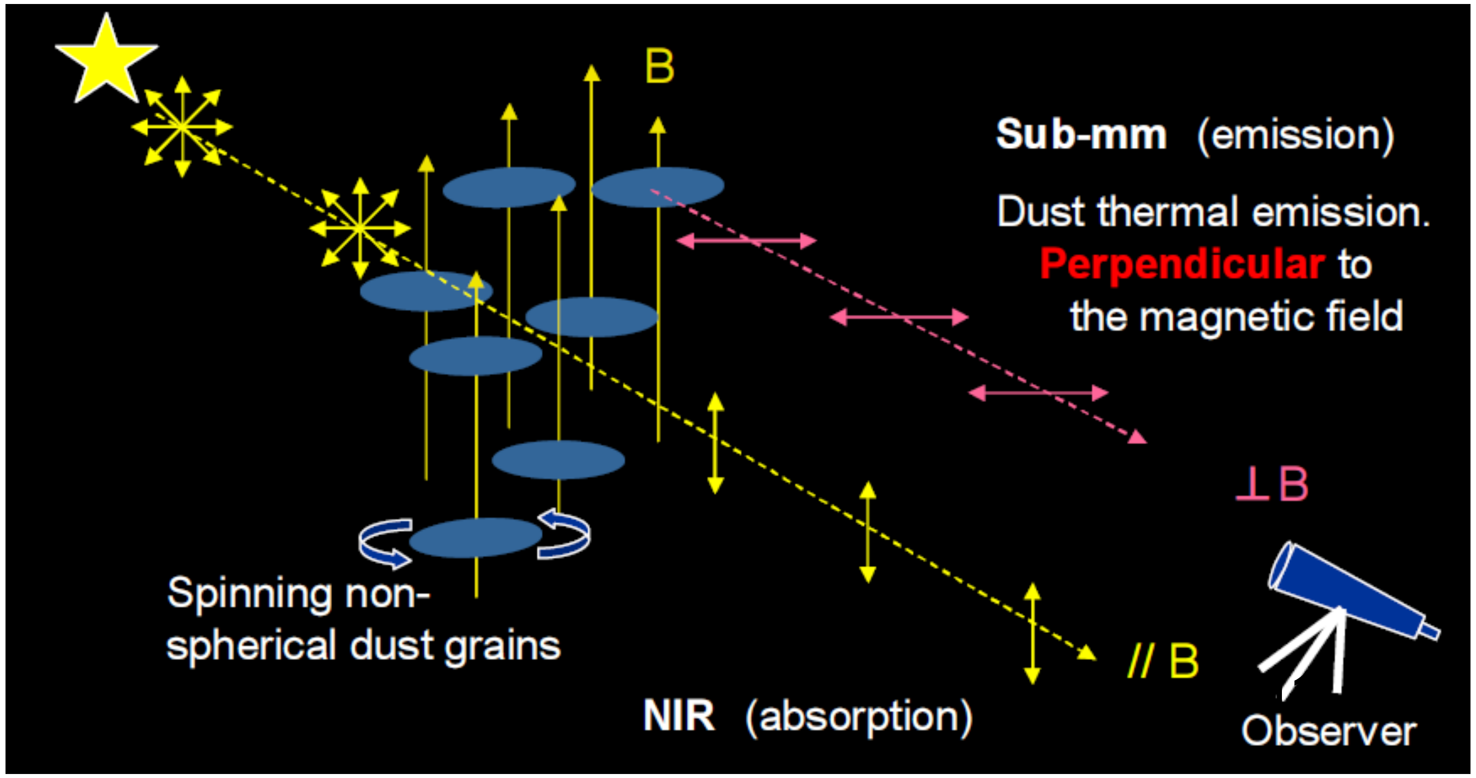

Figure courtesy: Tamara

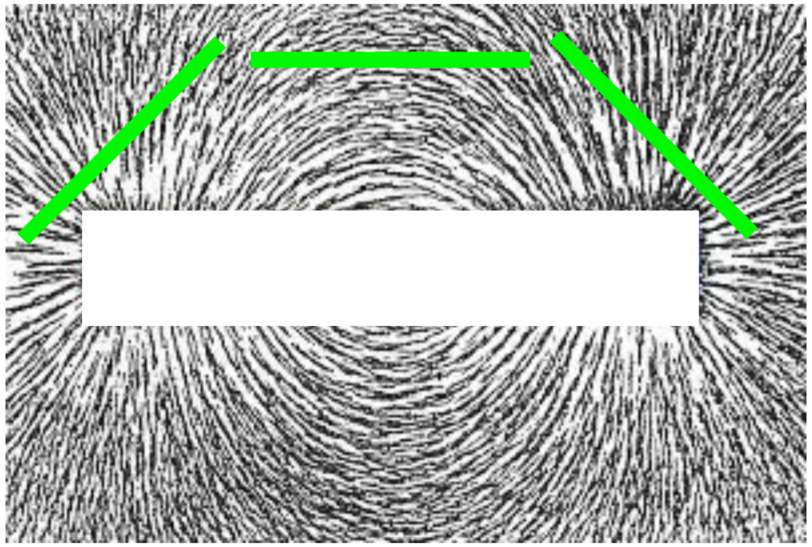

Orientation (segment)

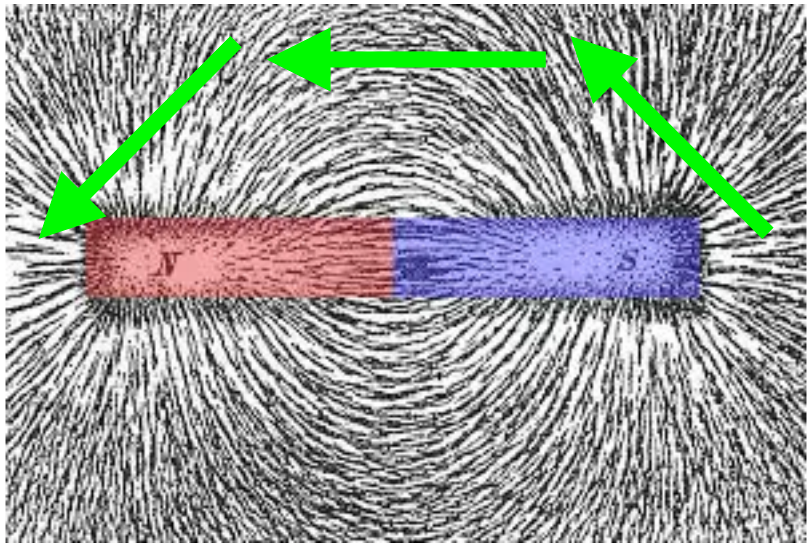

Direction (vector)

How to Determine B Field Direction?

ANALYSIS OF ZEEMAN EFFECT DATA IN RADIO ASTRONOMY

R. J. Sault, N. E. B. Killeen, J. Zmuidzinas, and R. Loushin
Astronomy Department, University of Illinois
Received 1989 October 9; accepted 1990 March 7

ABSTRACT

We discuss the analysis of Zeeman effect data in radio astronomy and in particular, extend previous techniques to include the case of low signal-to-noise ratios. We consider three statistical techniques for estimating the line-of-sight magnetic field: maximum likelihood, least-squares, and Wiener filters. For high signal-to-noise ratios, all three estimators are essentially unbiased. In the poor to moderate signal-to-noise ratio regime, we conclude that all three estimators are biased; the maximum likelihood technique yields results that are, in general, substantially less biased than least-squares and Wiener filters. However, it is possible to "debias" the least-squares results and obtain estimates that are as good as maximum likelihood under a restricted set of conditions.

"If the splitting was large enough that all three Zeeman components were well-separated, then the total magnetic field strength could be obtained from the measured separation of the split components."

LINEAR POLARIZATION OF INTERSTELLAR RADIO-FREQUENCY ABSORPTION LINES AND MAGNETIC FIELD DIRECTION

Nikolaos D. Kylafis
Institute for Advanced Study, Princeton
Received 1983 February 14; accepted 1983 May 5

ABSTRACT

It is predicted that interstellar radio-frequency absorption lines in the direction of H II regions, supernova remnants, and hot cores of molecular clouds are linearly polarized. The amount of linear polarization may be as large as several percent if (1) the optical depth is moderate and (2) the number of extrema of the velocity component along the line of sight through the absorbing medium is small. The polarization is caused by the linear dichroism of the interstellar medium, which in turn arises from the non-LTE population of the magnetic sublevels. Analytic expressions are presented for the amount of polarization expected in radio-frequency lines from absorbing material undergoing one-dimensional, two-dimensional axisymmetric, and three-dimensional isotropic collapse. A relation is given between the polarization vector and the magnetic field direction. This relation applies when the Zeeman splitting exceeds both the collisional frequency and the radiative transition rate.

"observations of linear polarization in radio-frequency absorption lines … are guaranteed to be informative."

Spectral-line Polarization: Goldreich-Kylafis Effect

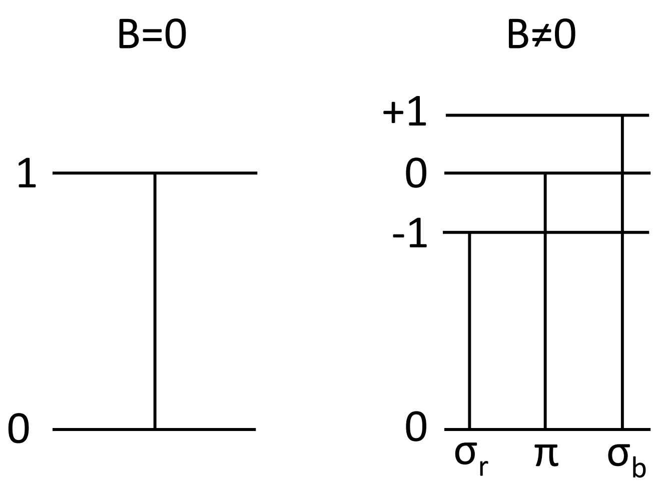

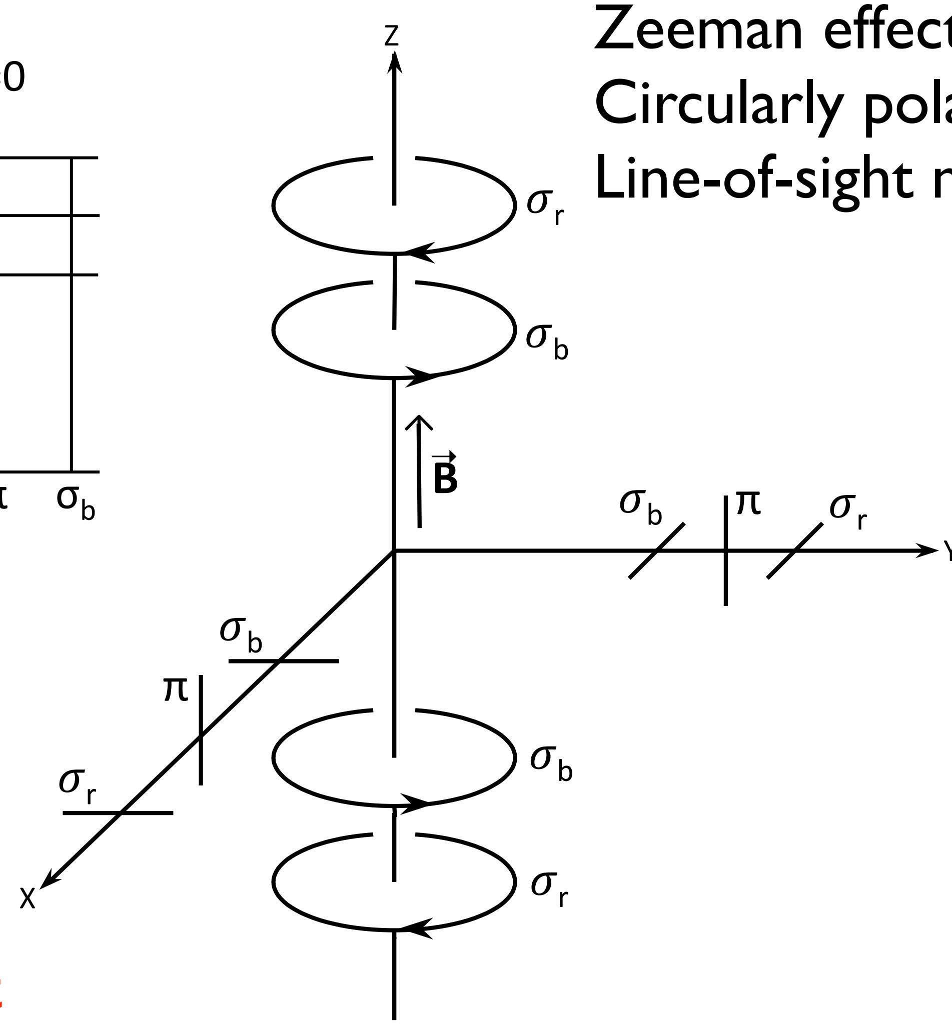

Zeeman effect
Circularly polarization
Line-of-sight magnetic field

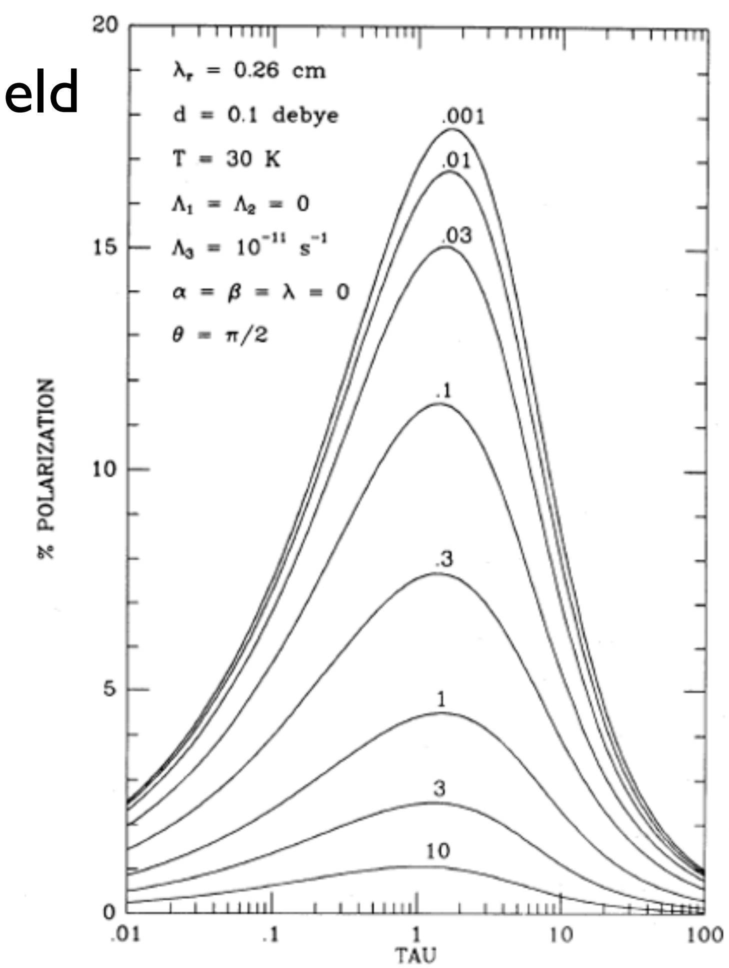

Goldreich-Kylafis Effect
Linearly polarization
Plane-of-sky magnetic field
Either parallel or perpendicular orientation

Crutceher & Kembell 2019

Kylafis et al. 1983

Goldreich-Kylafis Effect Observations

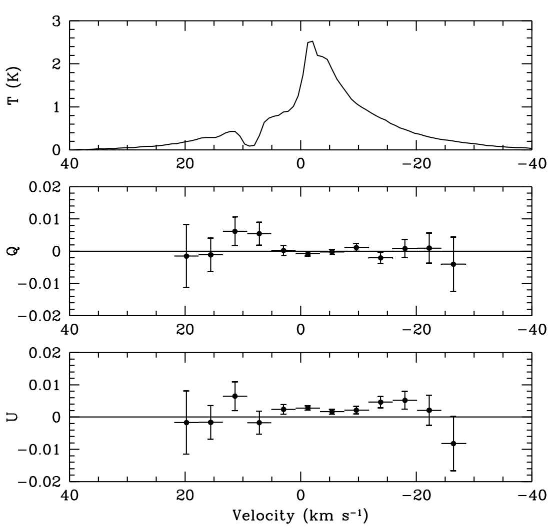

HCO+ 1-0, DR21
NRAO 12m, Glenn et al. 1997

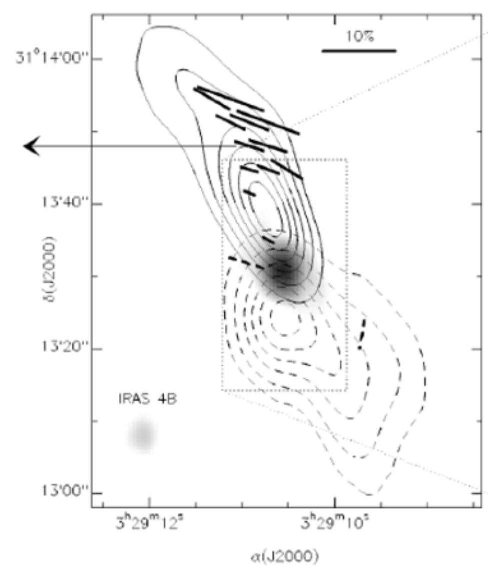

CO 2-1, NGC1333 IRAS4A
BIMA, Girart et al. 1999

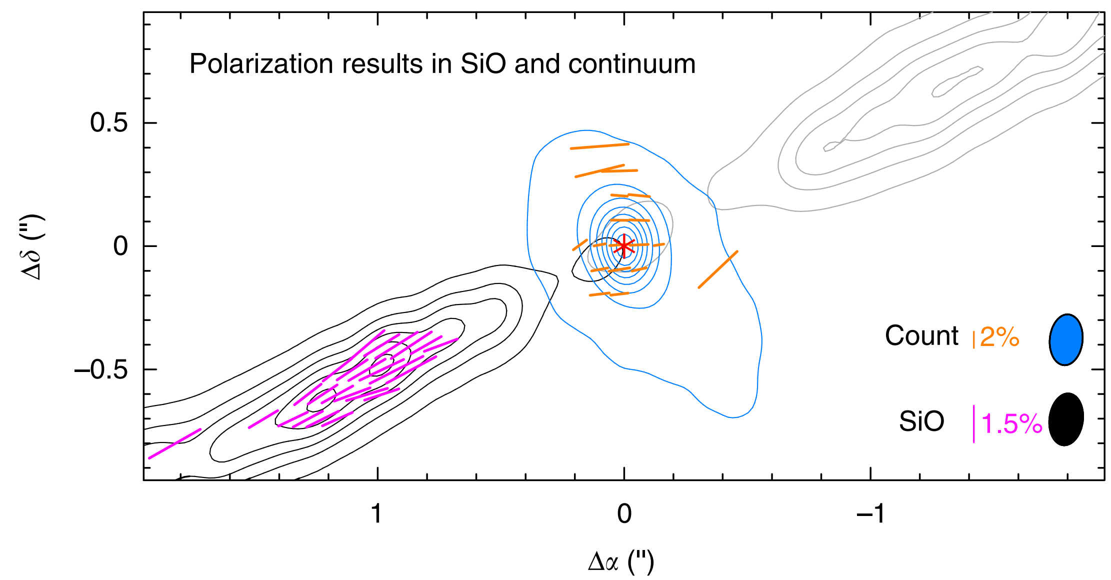

SiO 8-7, HH211
ALMA, Lee, Huang, Ching et al. 2018

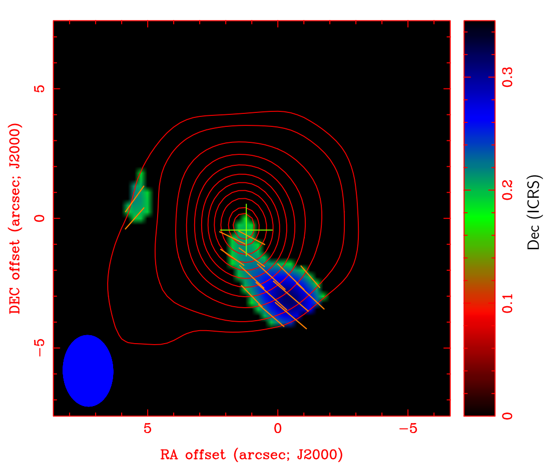

SiS 19-18, IRC+10216
SMA, Girart et al. 2012

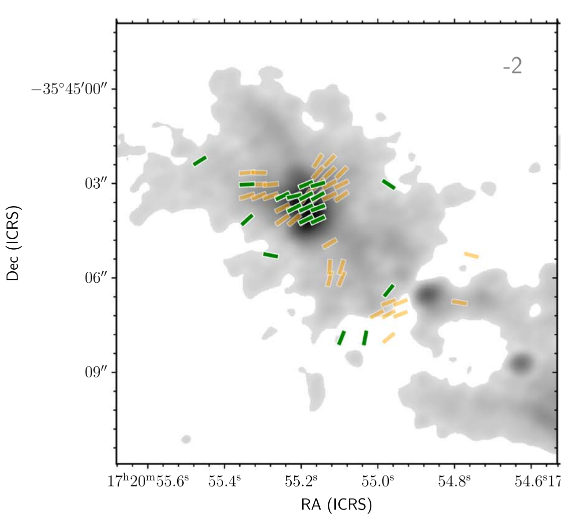

CS C^{33}S 5-4, NGC 6334I(N)
ALMA, Cortes et al. 2021

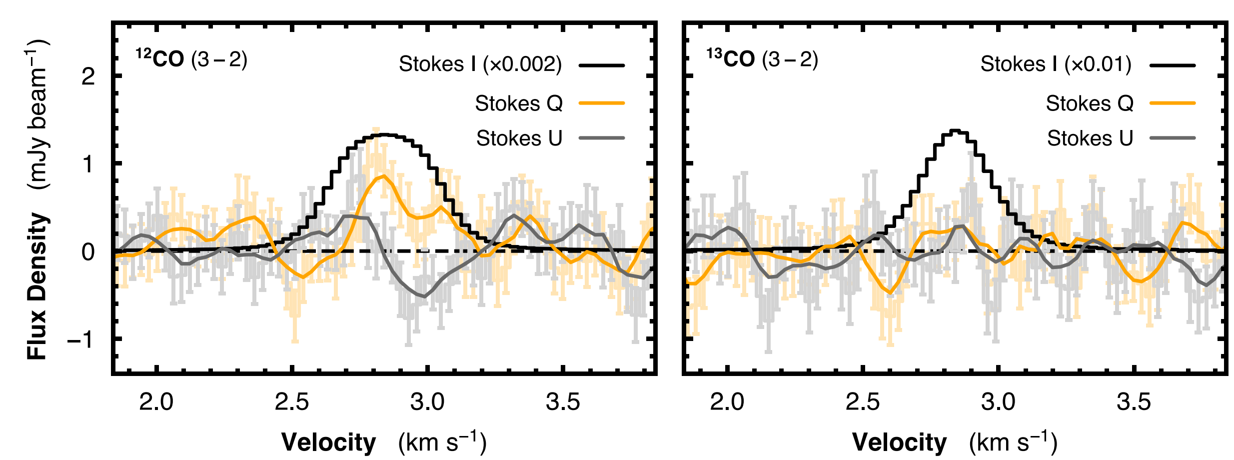

CO 3-2, ^{13}CO 3-2, TW Hya
ALMA, Teague et al. 2021

SMA Observations in NGC1333 IRAS4A

- 1.2 $M_\odot$ Class 0 protostellar binary 4A1 & 4A2 with prominent outflows
- A text-book example of magnetic dominated star formation

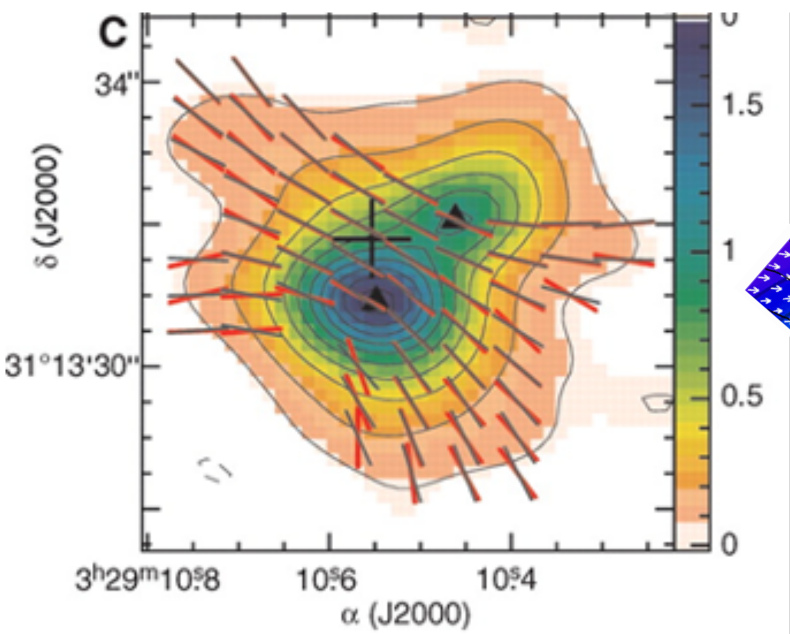

dust polarization
Girart et al. 2006

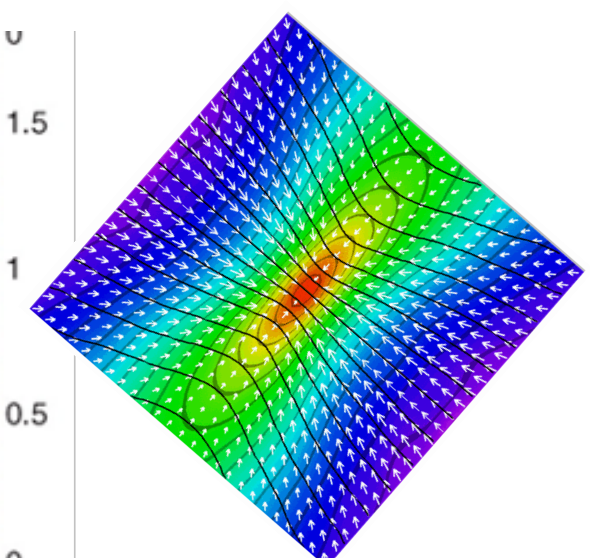

MHD model
Fiedler & Mouschovias 1993

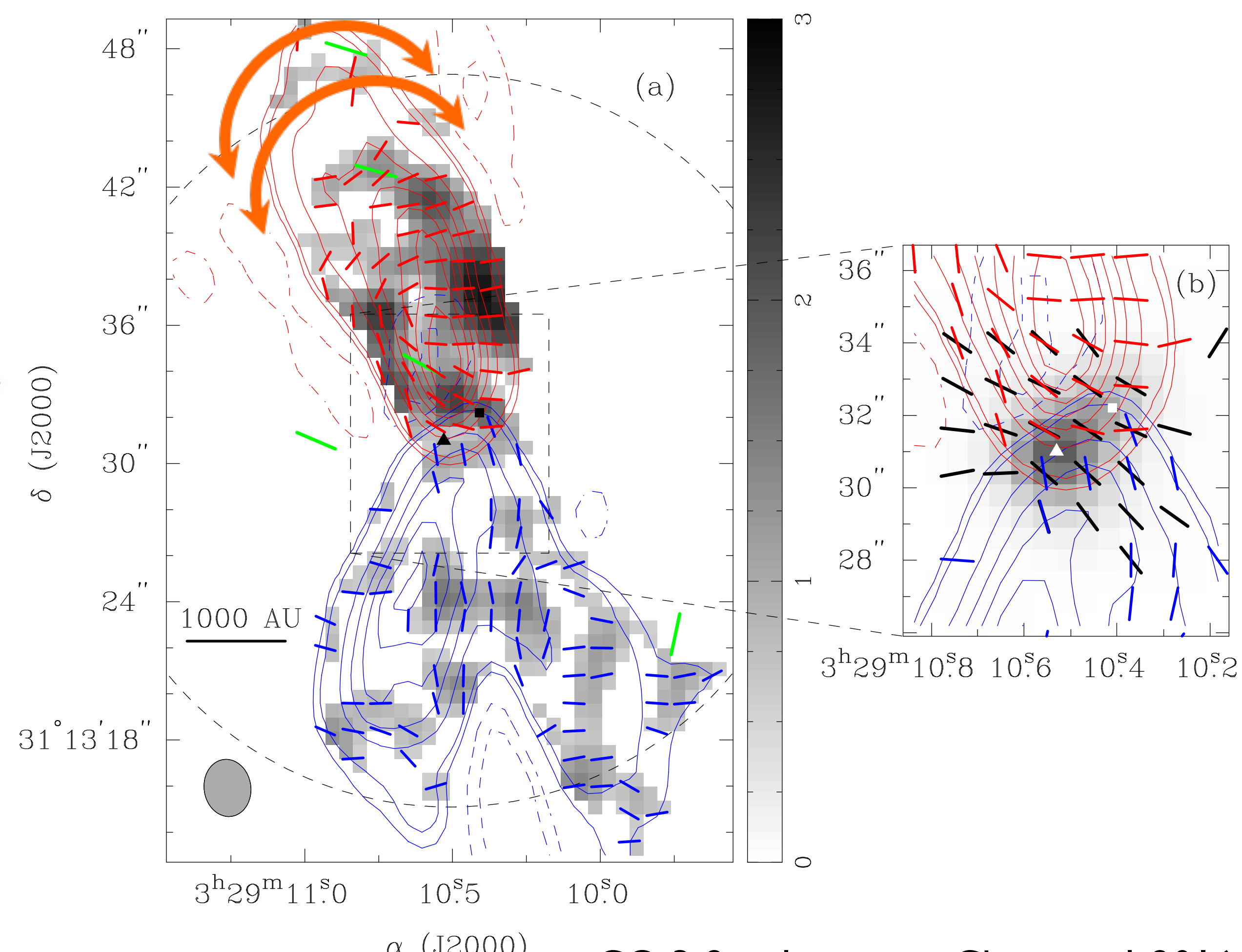

CO 3-2 polarization, Ching et al. 2016

ALMA CO 2-1 Polarization Observations

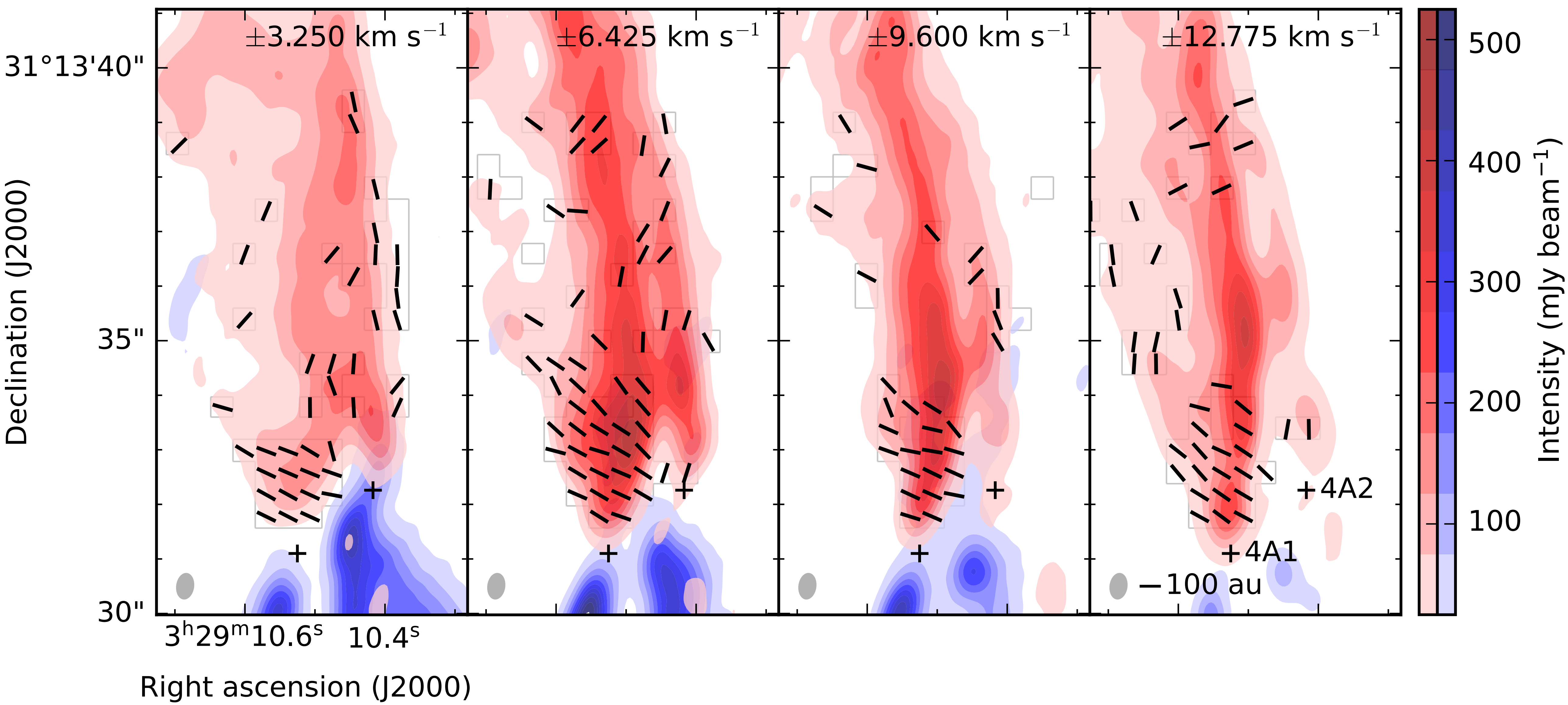

ALMA CO 2-1 Polarization Observations

CO vs dust polarization

CO moment1

(Intensity-weighted mean velocity)

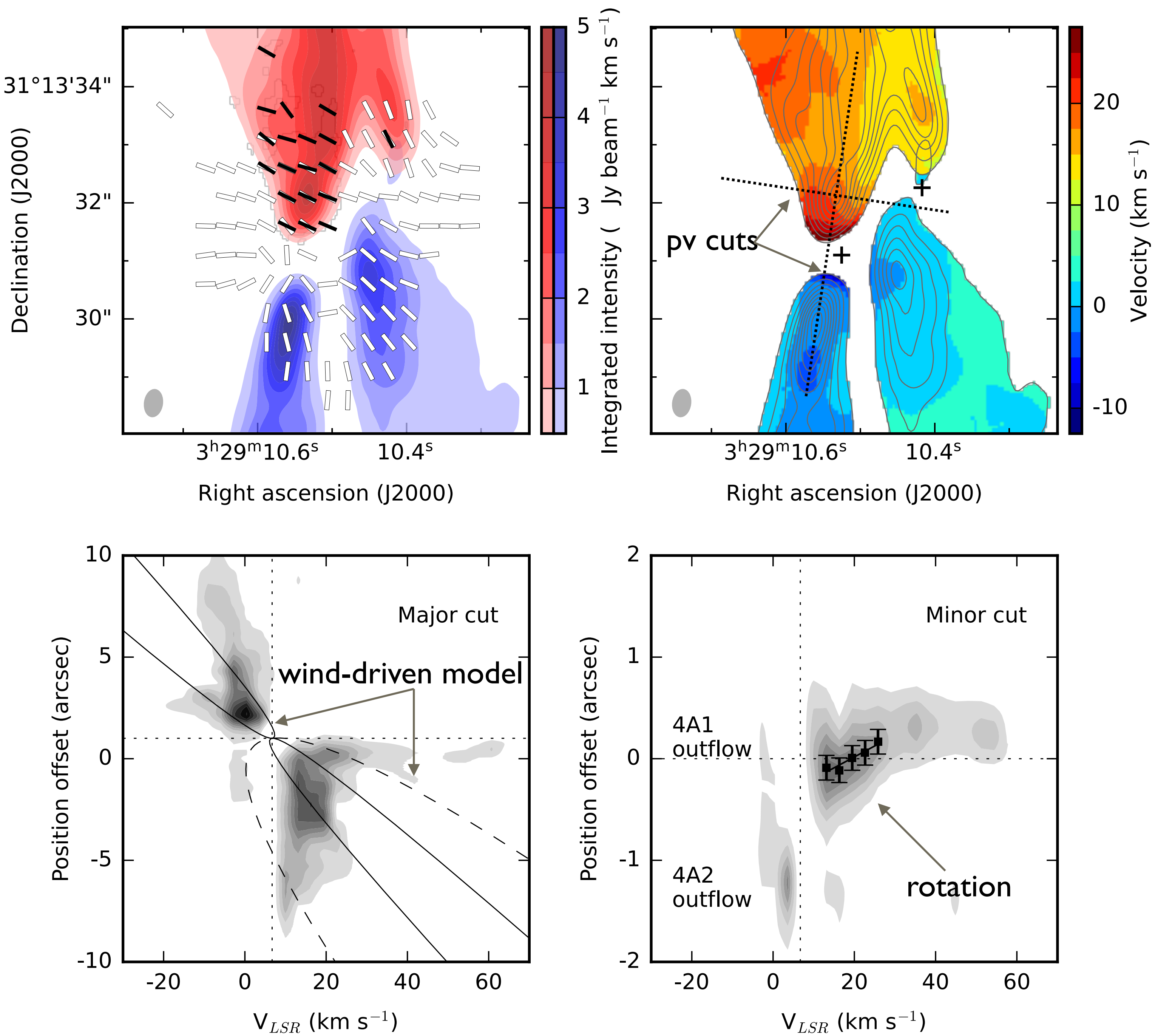

PV diagram major cut

PV diagram minor cut

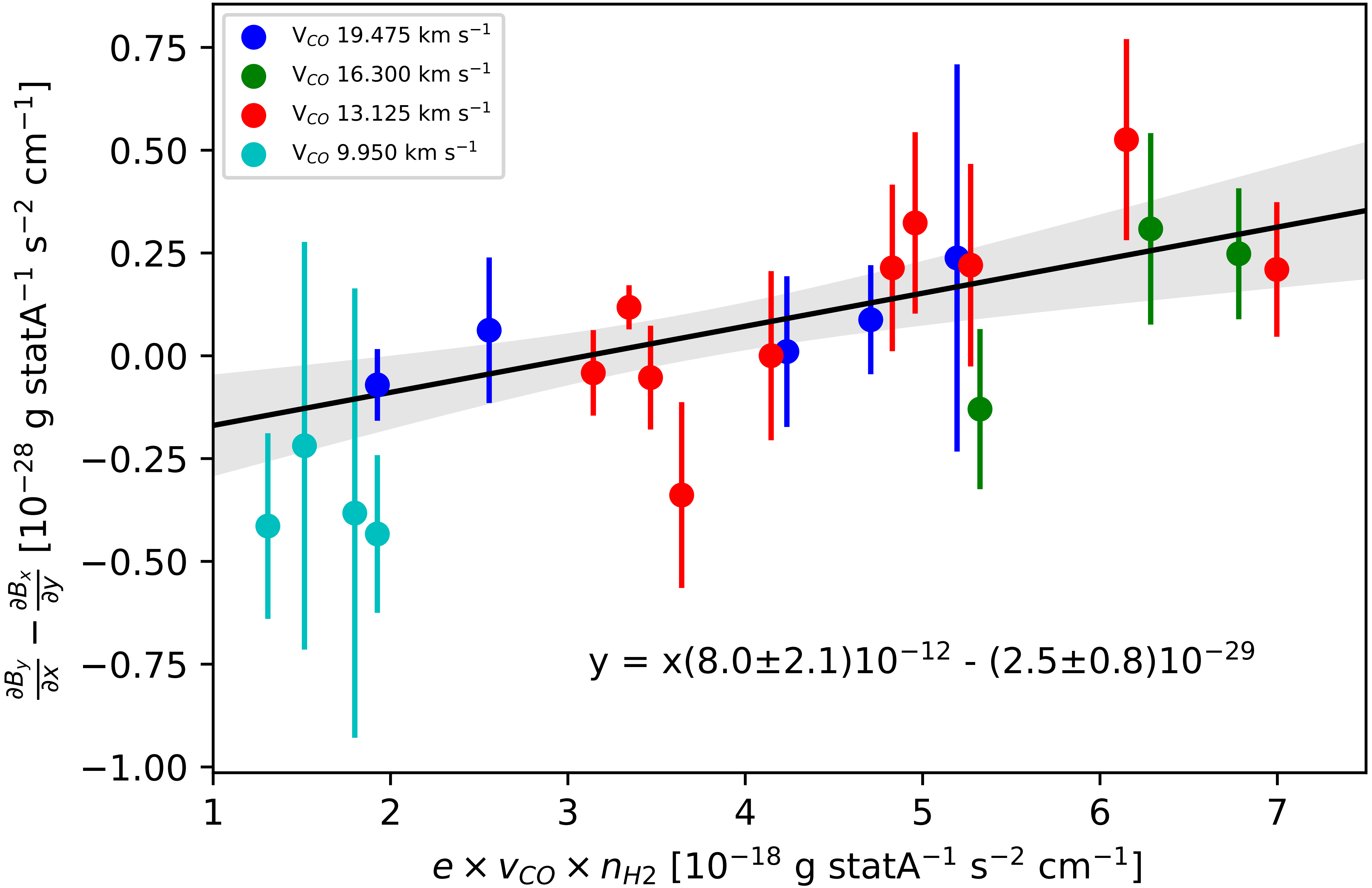

$$\frac{\partial B_y}{\partial x} - \frac{\partial B_x}{\partial y} = \mu_0 J_z + \mu_0 \epsilon_0 \frac{\partial E_z}{\partial t}$$

$$J_z = e \times n_e \times v_e = e \times (n_{H2} X_e) \times (v_{CO} X_v)$$

$$\boxed{X_e X_v = 8.0 \times 10^{-12}}$$

Xe and Xv

- In theory, Xe ~ 10^{-7}-10^{-8}, Xv ~ 10^{-2}-10^{-3}
- In observation, Xe ~ 10^{-6}-10^{-8} (Caselli et al. 1998), Xv < 10^{-1} at 100 au (Yen et al. 2018)

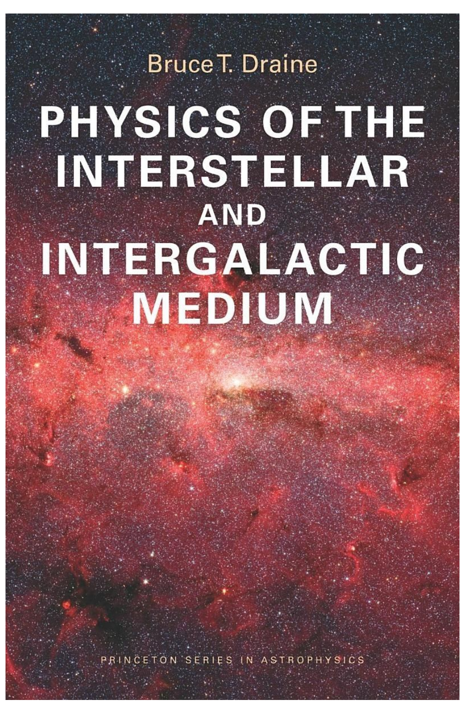

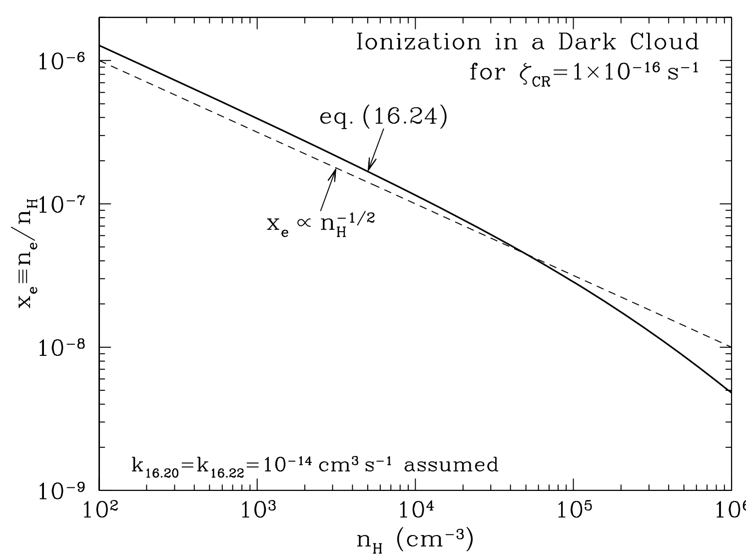

Figure 16.3 Fractional ionization in a dark cloud, estimated using Eq. (16.25), with the grain recombination rate coefficients set to $k_{16.20} = k_{16.22} = 10^{-14}\,\mathrm{cm}^3\,\mathrm{s}^{-1}$ (see Fig. 14.6). The dashed line is a simple power-law approximation $x_e \approx 1 \times 10^{-5}(n_\mathrm{H}/\mathrm{cm}^{-3})^{-1/2}$.

$$(\mathbf{v}_i - \mathbf{v}_n) = -\frac{(m_i + m_m)}{m_i m_n}\frac{1}{n_i n_n \langle\sigma v\rangle}\nabla\frac{B^2}{8\pi} \quad . \tag{41.55}$$

Suppose that a clump has characteristic magnetic field strength B and characteristic dimension L (see Figure 41.1). The time scale for the magnetic field to slip out of the clump is

$$\tau_\mathrm{slip} = \frac{L/2}{|\mathbf{v}_i - \mathbf{v}_n|} = \frac{8\pi(L/2)^2}{B^2} n_i n_n \langle\sigma v\rangle \frac{m_i m_n}{(m_n + m_i)} \quad . \tag{41.56}$$

where we have approximated $\nabla B^2 \approx B^2/(L/2)$. To evaluate this, suppose that (1) $L \approx 1.23 n_4^{-0.81}$ pc (Eq. 32.12), (2) the magnetic field strength is given by the observed relation $B \approx 49 n_4^{0.65}\,\mu$G for the median field strength [Eq. (32.17)], and (3) the fractional ionization $n_i/n_\mathrm{H} \approx 1 \times 10^{-7} n_4^{-1/2}$ (see Fig. 16.3). Then,

$$\tau_\mathrm{slip} \approx 7 \times 10^7 n_4^{-1.42}\,\mathrm{yr} \quad . \tag{41.57}$$

B Vector Map

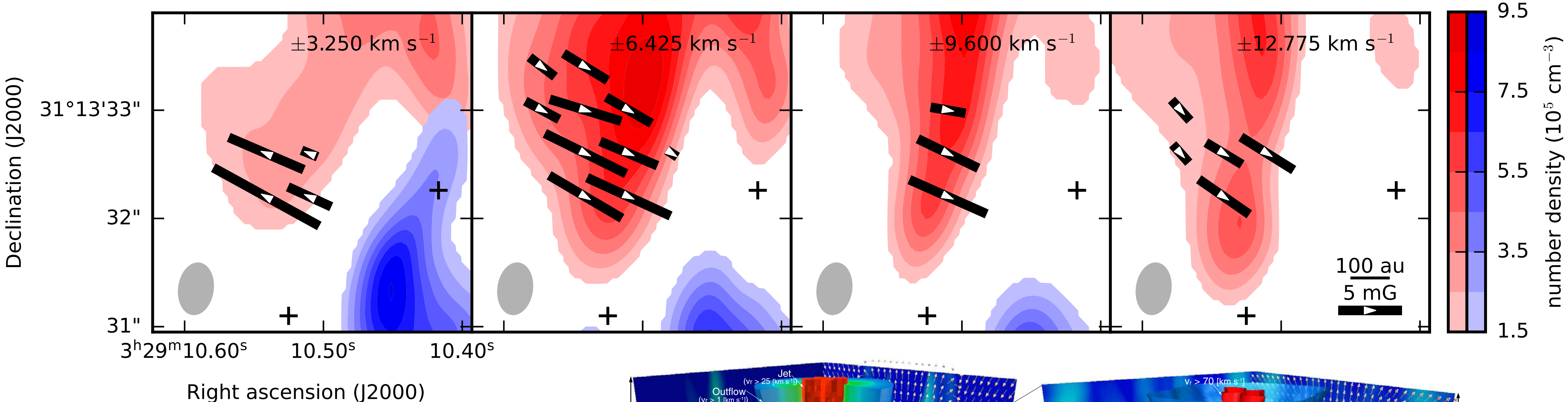

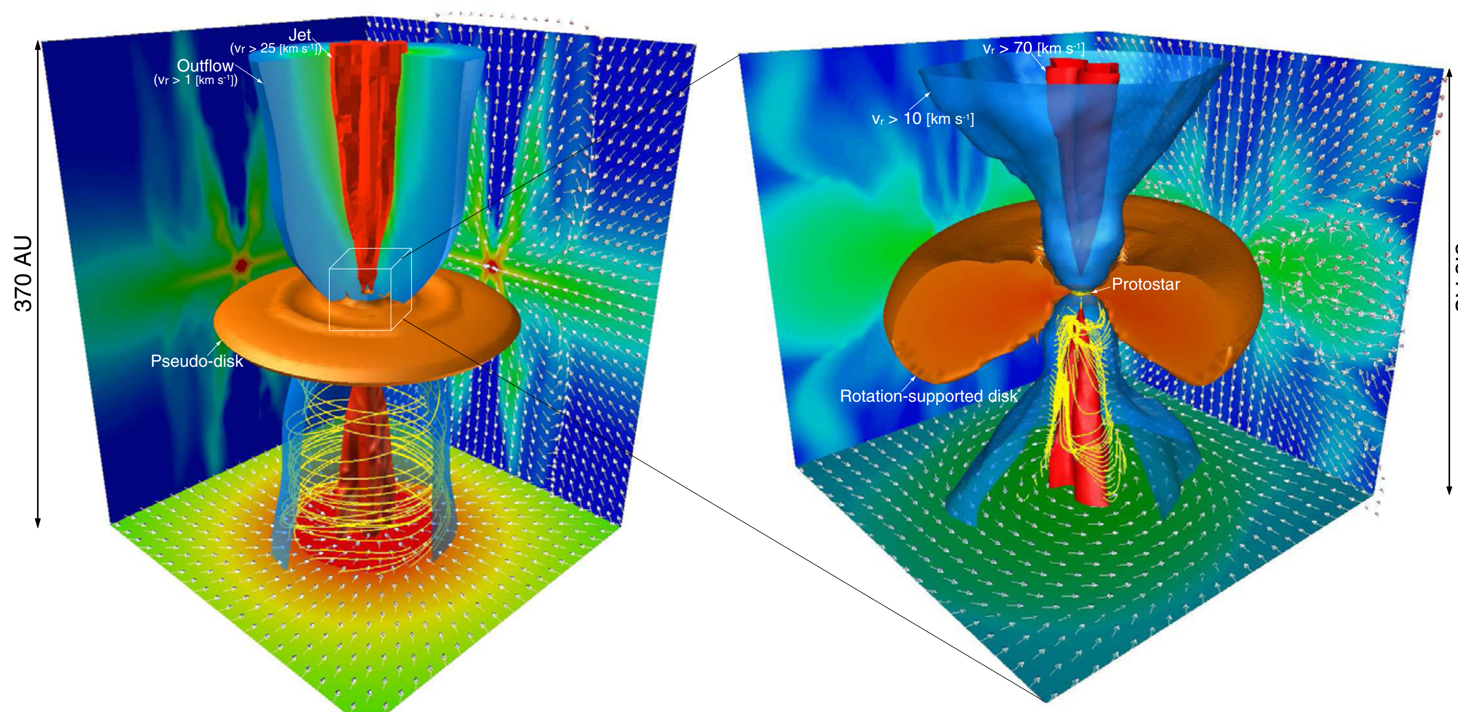

Machida et al. 2008; Machida 2014

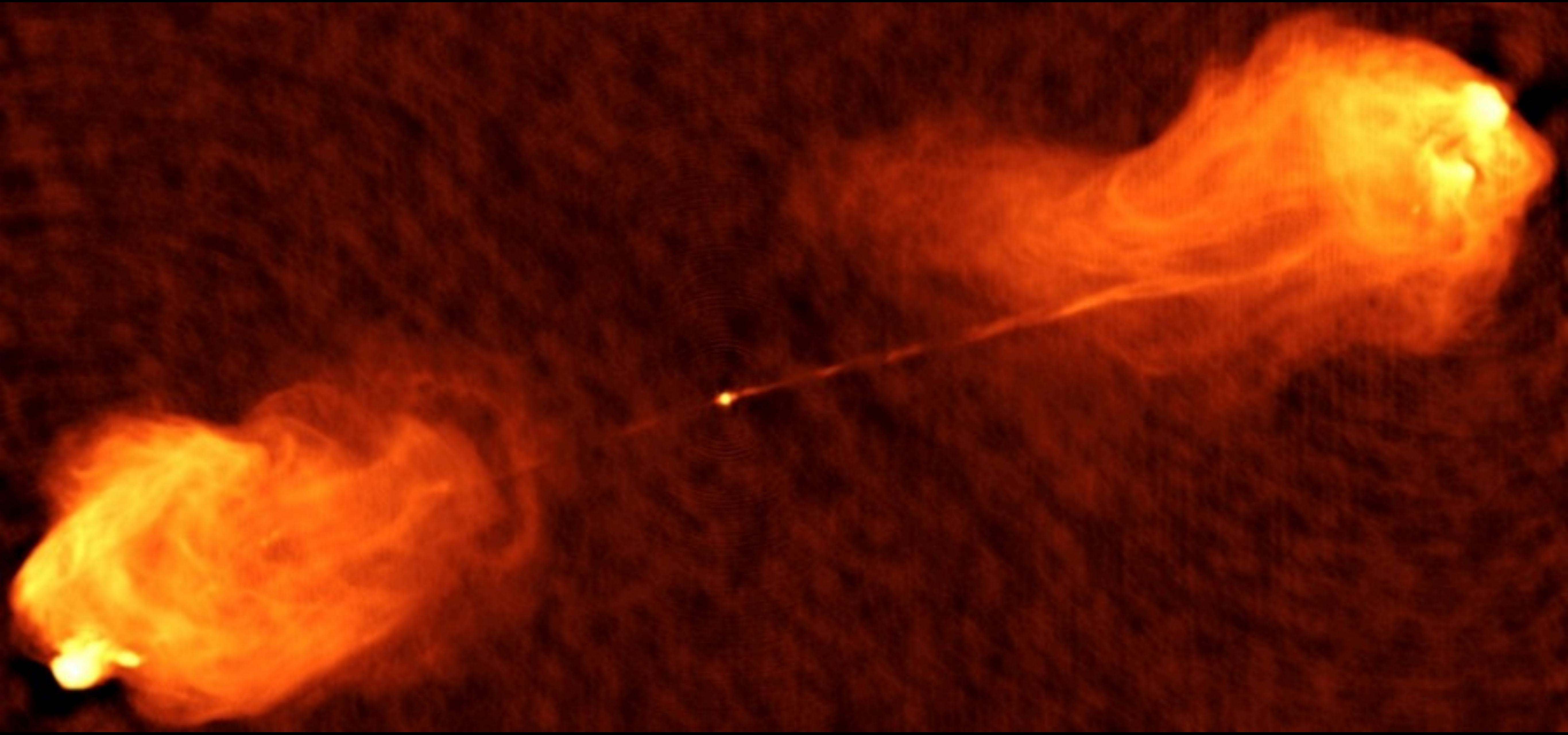

Image credit: NRAO

Tracing Magnetic Field in Molecular Jet-Driving Galactic Nucleus 2018.1.00695.S

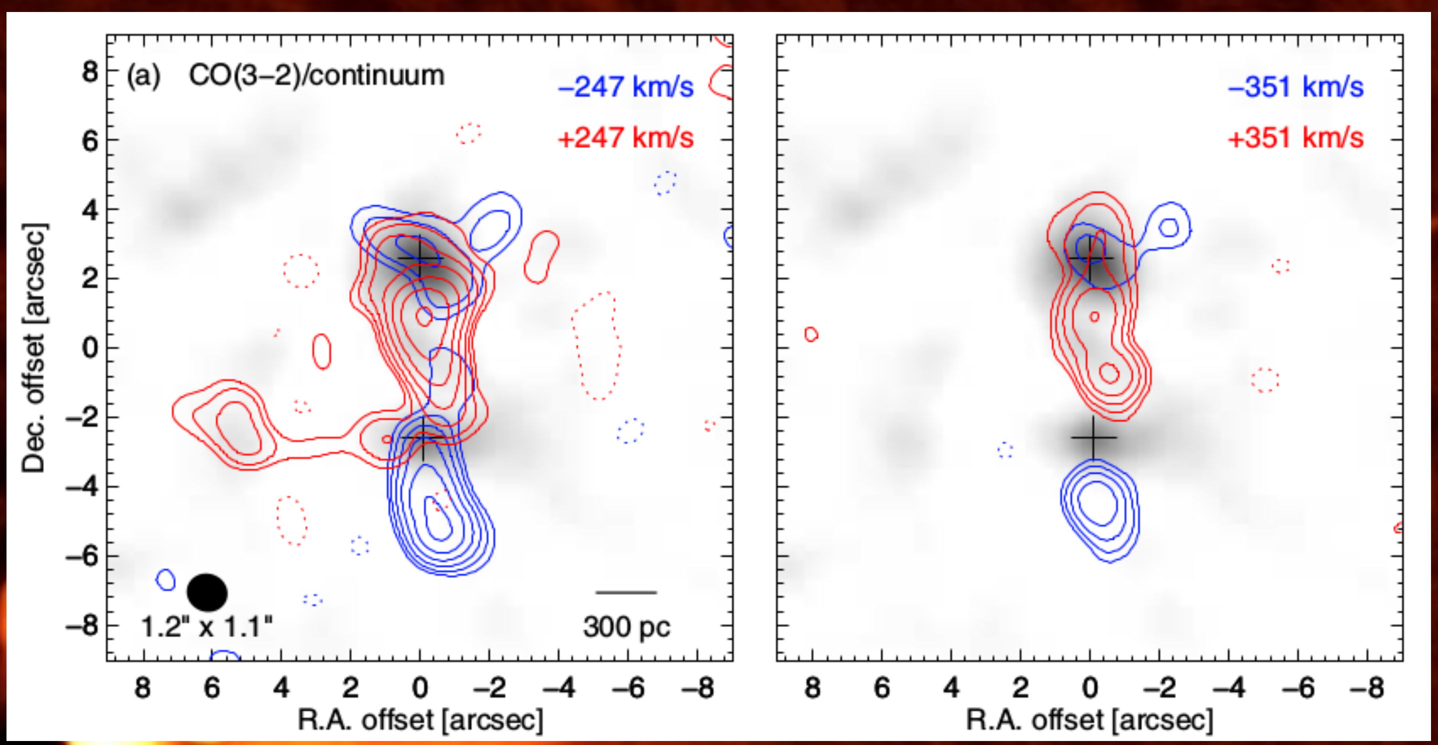

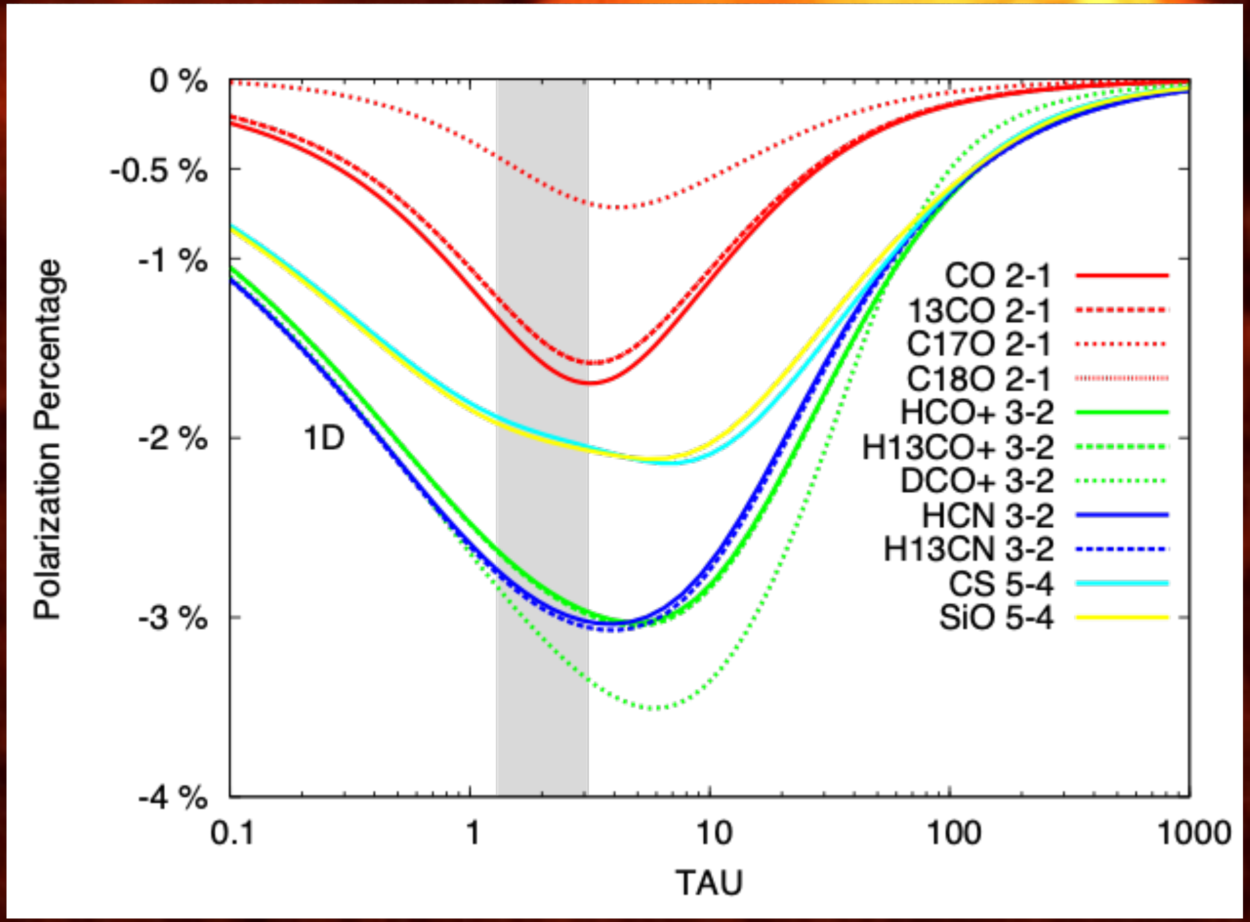

ALMA proposal: Hauyu Baobab Liu; Tao-Chung Ching; Sergio Martin

Image credit: NRAO

Goldreich-Kylafis Effect Calculations

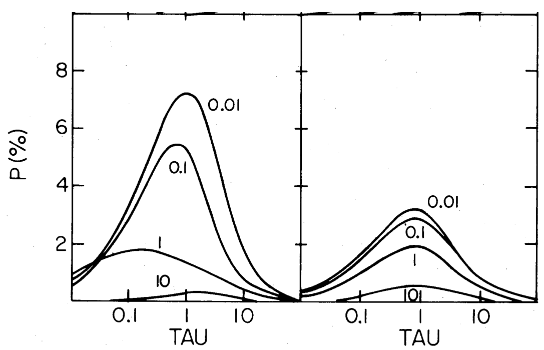

Deguchi & Watson 1984

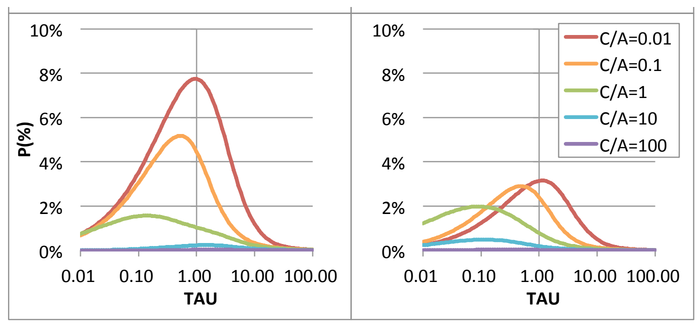

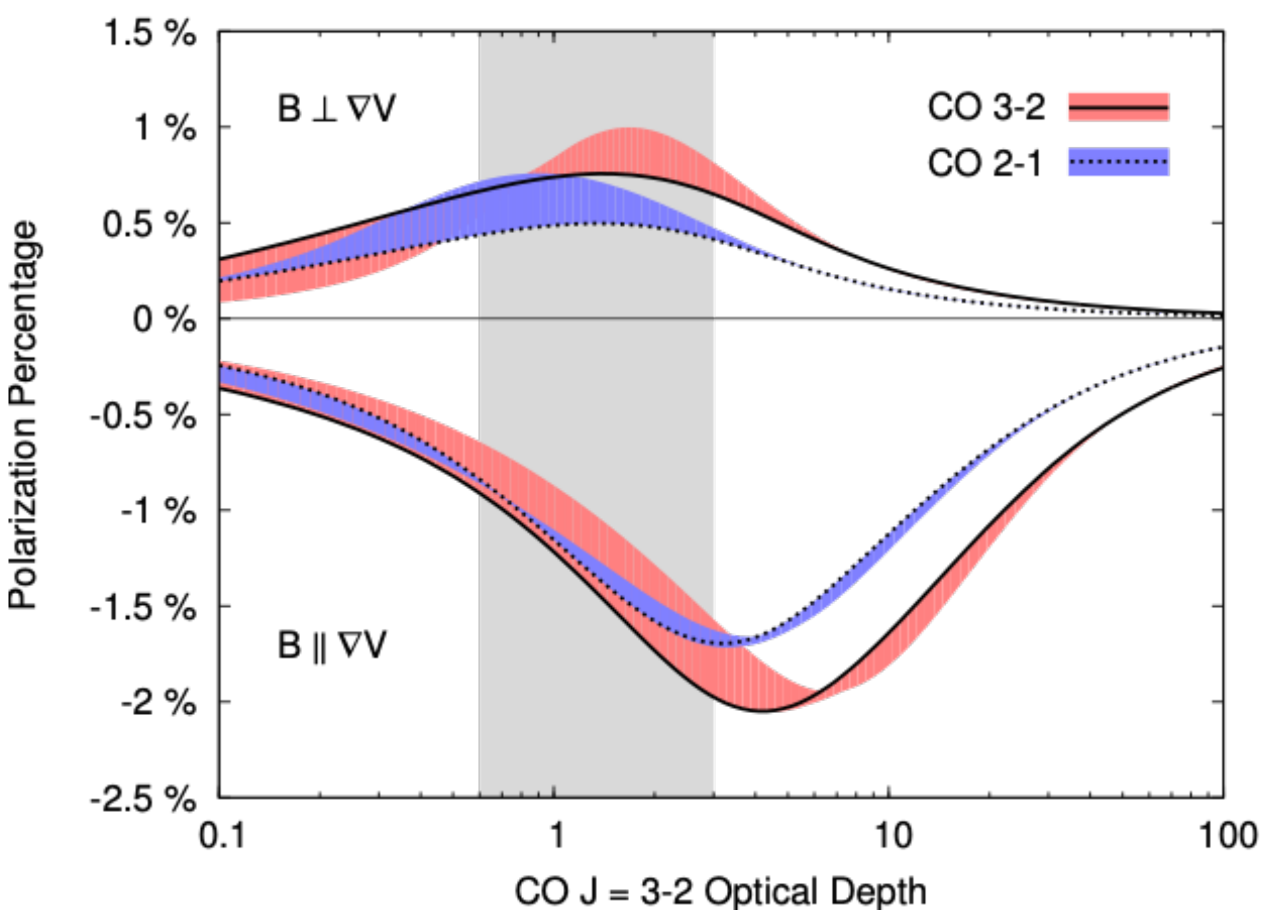

Ching et al. 2016

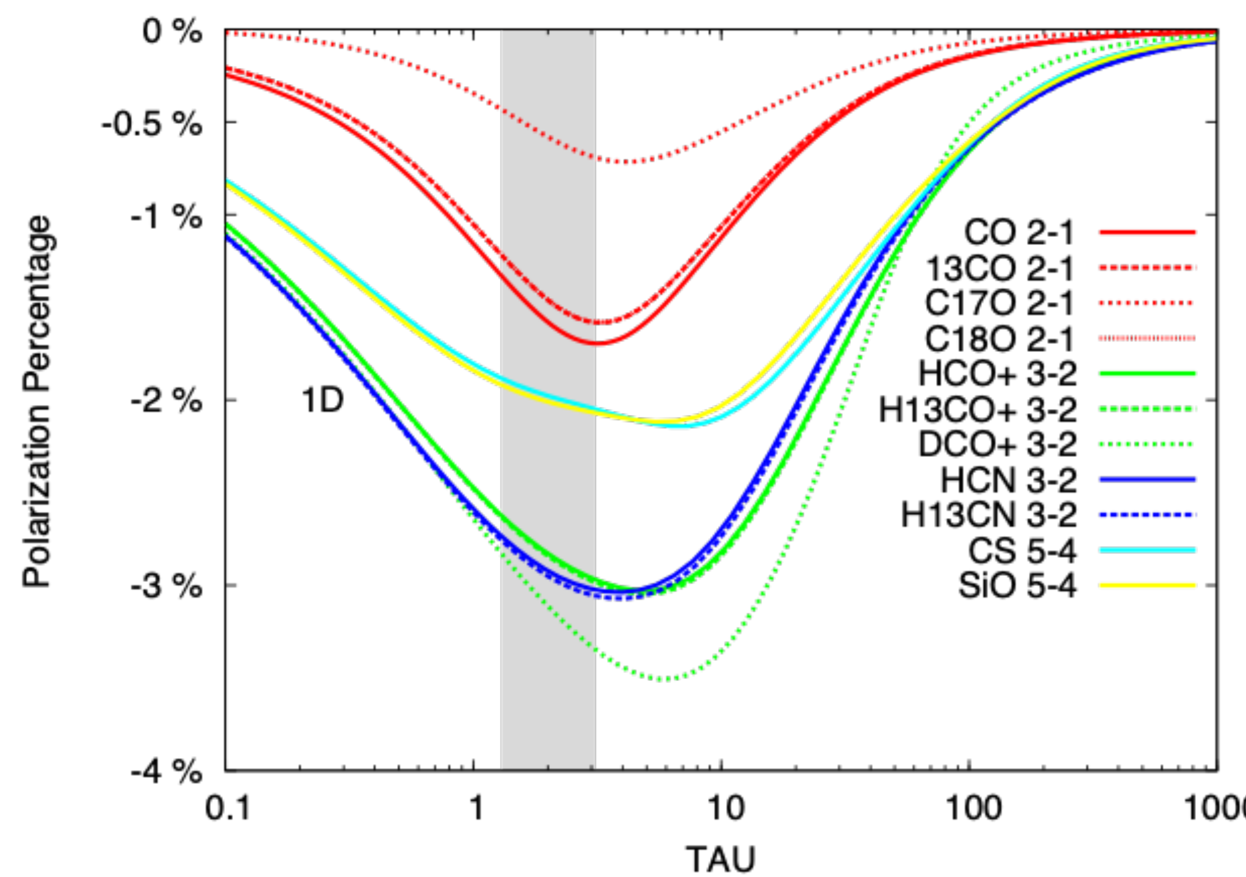

Correlation of Ampere Law in HI data?

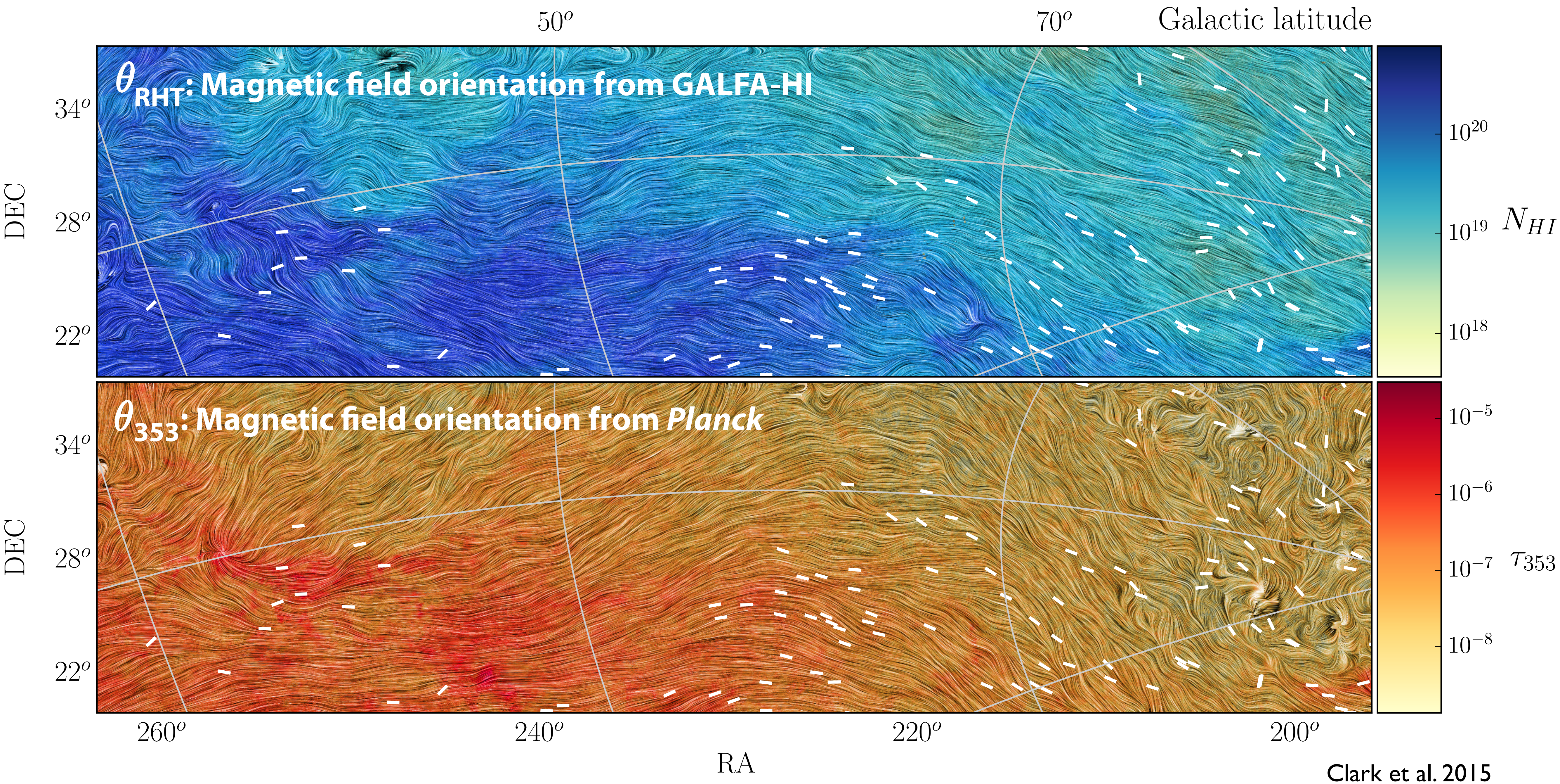

Clark et al. 2015

No V_{CO}, drift velocity = 1 m/s

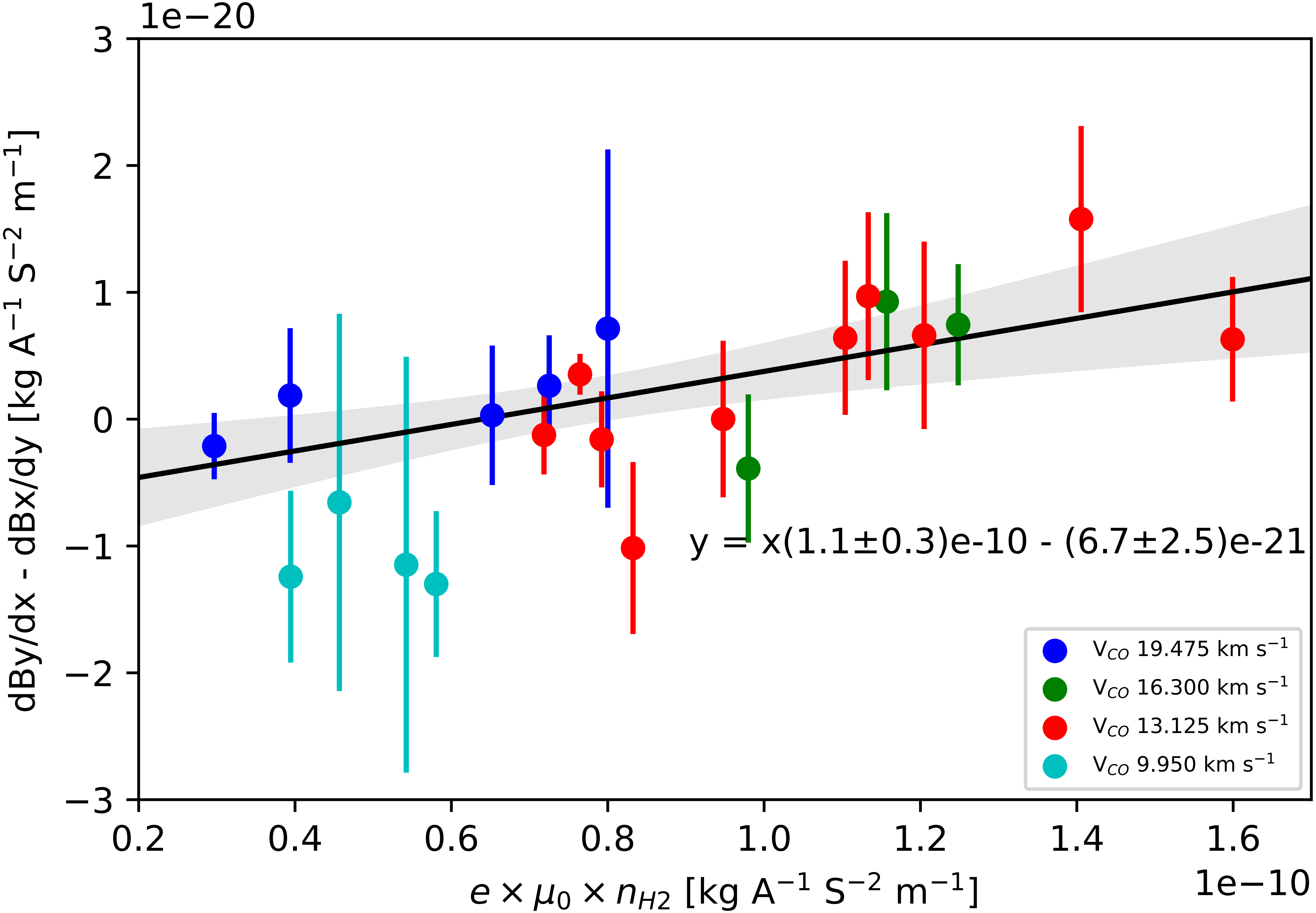

check sqrt(n_{H2}) dependance in B